

DC-transport in superconducting point contacts: a full counting statistics view

J.C. Cuevas

Institut für Theoretische Festkörperphysik, Universität Karlsruhe, D-76128 Karlsruhe, Germany

W. Belzig

Department of Physics and Astronomy, University of Basel, Klingelbergstr.82, CH-4056 Basel, Switzerland

(Dated: April 14, 2004)

We present a comprehensive theoretical analysis of the dc transport properties of superconducting point contacts. We determine the full counting statistics for these junctions, which allows us to calculate not only the current or the noise, but all the cumulants of the current distribution. We show how the knowledge of the statistics of charge transfer provides an unprecedented level of understanding of the different transport properties for a great variety of situations. We illustrate our results with the analysis of junctions between BCS superconductors, contacts between superconductors with pair-breaking mechanisms and short dissipative bridges. We also discuss the temperature dependence of the different cumulants and show the differences with normal contacts.

PACS numbers: 74.50.+r, 72.70.+m, 73.23.-b

I. INTRODUCTION

The current-voltage (I-V) characteristics of superconducting contacts have been the subject of investigation during the last four decades. The first experimental analyses were performed in tunnel junctions [1]. In this case the current inside the superconducting gap is suppressed, and the results can be accurately described with the BCS theory [2]. However, very often a significant current is observed in the subgap region, which cannot be explained with the simple tunnel theory. The first anomalies were reported by Taylor and Burstein [3] who noticed a small onset in the current when the applied voltage V was equal to the energy gap, $=e$, in a tunneling experiment between two equal superconductors. Relatively soon afterwards it was apparent [4, 5] that not only is there an anomaly in the current at $eV = \Delta$, but in fact at all submultiples $2\Delta/n$, where n is an integer. This set of anomalies is referred to as subhamonic gap structure (SGS), and its temperature and magnetic field dependence were thoroughly characterized [6, 7, 8].

The first theoretical attempt to explain the SGS was done by Schrieffer and Wilkins [9], who noticed that if two electrons could tunnel simultaneously, this process would become energetically possible at $eV = \Delta$, and cause the structure in the I-V observed by Taylor and Burstein [3]. Within this multiparticle tunneling theory the origin of the SGS would be the occurrence of multiple processes in which n quasiparticles cross simultaneously the contact barrier. The original perturbative analysis of this theory has serious problems. In particular, the current was found to diverge at certain voltage, which avoids to calculate meaningful I-Vs within this approach. A second explanation was put forward by Werthamer [10], who suggested that the SGS could be caused by a self-detection of the ac Josephson effect. The main problem of this explanation is that it invokes two different mechanisms for the odd and even terms, while the experimental current jumps are identical for both series. In 1982 Klap-

wijk, Blonder and Tinkham [11] introduced the concept of multiple Andreev reflection (MAR). In this process a quasiparticle undergoes a cascade of Andreev reflections in the contact interface (see Fig. 1). They showed that a MAR in which a quasiparticle crosses the interface n times becomes possible at a voltage $eV = 2\Delta/n$, which explains naturally the SGS. The quantitative analysis of the I-Vs was based on a semiclassical approach which fails away from perfect transparency [12, 13]. A few years later, Arnold reported the first fully microscopic calculation of I-Vs based on a Green's function approach [14].

The theoretical discussion was finally clarified with the advent of modern microscopic theories. Using the scattering formalism [15, 16, 17] and the so-called Hamiltonian approach [18], different authors reported a complete analysis of the dc and ac Josephson effect in point contacts. These theories clearly showed that the MARs are responsible of the subgap transport in these systems. They also showed that the multiparticle tunneling of Schrieffer and Wilkins and the MARs are indeed the same mechanism. The new microscopic theories have also allowed the calculation of a series of properties such as resonant tunneling [19, 20], shot noise [21, 22] and the Shapiro steps [23].

From the experimental point of view, the main problem has always been the proper characterization of the interface of the superconducting contact. Uncertainties in the interfaces properties often avoid a proper comparison between theory and experiment. The situation has considerably improved with the appearance of the metallic atomic-sized contacts, which can be produced by means of scanning tunneling microscope and break-junction techniques [24, 25, 26, 27, 28, 29, 30, 31, 32]. These nanowires have turned out to be ideal systems to test the modern transport theories in microscopic superconductors. Thus, for instance Scheer and coworkers [28] found a quantitative agreement between the measurements of the current-voltage characteristics of different atomic contacts and the predictions of the theory for a single-channel superconducting contact [16, 18]. These

experiments not only helped to clarify the origin of the SGS, but also showed that the set of the transmission coefficients in an atomic-size contact is amenable to measurement. This possibility has recently allowed a set of experiments that confirm the theoretical predictions for transport properties such as supercurrent [31], noise [32] and even resonant tunneling in the context of carbon nanotubes [33]. From these combined theoretical and experimental efforts a coherent picture of transport in superconducting point contacts has emerged with multiple Andreev reflections as a central concept.

The most recent development in the understanding of the dc transport in superconducting contacts is the analysis of the full counting statistics [34, 35]. Full counting statistics (FCS) is a familiar concept in quantum optics (see for instance [36]), which has been recently adapted to electron transport in mesoscopic conductors by Levitov and coworkers [37]. FCS gives the probability $P(N)$ that N charge carriers pass through a conductor in the measuring time. Once these probabilities are known one can easily compute not only the mean current and noise, but all the cumulants of the current distribution. Since the introduction of FCS for electronic systems, the theory has been sophisticated and applied to many different contexts (see Ref. [38] for a recent review).

The counting statistics of a one-channel quantum contact has the surprisingly simple form of a binomial distribution $P(N) = \binom{M}{N} T^N (1-T)^{M-N}$, where T is the transmission probability and $M = V$ is the number of attempts [37, 39]. The generalization to many contacts and/or finite temperatures is straightforward, by noting that different energies and channels have to be added independently. In this way, the counting statistics of diffusive contacts at zero temperature [40] and at finite temperatures [41] could be obtained using the universal distribution of transmission eigenvalues [42, 43]. It is worth to note, that the FCS in the limit of small transparency reduces to a Poisson distribution, which can also be obtained using classical arguments and neglecting correlations between the different transfer events. Interestingly, the Poissonian character allows to directly extract the charge of the elementary event, which can be used to determine e.g. fractional charges [44, 45, 46]. A general approach to obtain the counting statistics of mesoscopic conductors was formulated by Nazarov [41] using an extension of the Keldysh-Green's function method, which allowed to present the counting statistics of a large class of quantum contacts in a unified manner [47]. In Ref. [34] we have shown, how this method can be used for a time-dependent transport problem like a superconducting contact out of equilibrium.

The counting statistics of a contact between a normal metal and a superconductor at zero temperature and $eV \ll E_{Th}$ was shown to be again binomial with the important difference that only even numbers of charges are transferred [48]. The probability of an elementary event is then given by the Andreev reflection coefficient $R_A = T^2/(2 - T^2)$ [49]. Again, the generalization of this

result to many channel conductors is obtained by summing over independent channels. For a diffusive metal the resulting statistics was shown to be an exact replica of the corresponding statistics for normal diffusive transport, provided the double charge transfer is taken into account [50]. This holds for coherent transport $eV \ll E_{Th}$, where E_{Th} is the inverse diffusion time, as well as in the fully incoherent regime $eV \gg E_{Th}$ [51]. For intermediate voltages, correlations of transmission eigenvalues at different energies modify the distribution of transmission eigenvalues [52], which lead to a nonuniversal behavior of the transport statistics, predicted theoretically [53] and confirmed experimentally [54]. Here, we note that a doubling of the noise was experimentally observed in diffusive wires [55], confirming earlier theoretical predictions [56]. However, to trace this back to a doubling of the elementary charge transfer follows only from an analysis of the counting statistics. A direct experimental determination of the doubled charge transfer was recently performed in a conductor containing a tunnel junction [57]. Here, the underlying statistics is Poissonian and the noise directly gives access to the charge of the elementary event [58, 59].

An interesting problem occurs, when one applies the concept of counting statistics to a supercurrent through a quantum contact [47]. The resulting statistics can not be directly related to a probability distribution, since some of the 'probabilities' would be negative. A closer inspection of the formalism showed, that the interpretation of probabilities relies on the proper definition of a quantum measuring device [60, 61, 62]. As we will see below, in superconducting contacts out of equilibrium these problems do not occur and all probabilities are positive.

In Ref. [34] we have demonstrated that the charge transport in superconducting point contacts out of equilibrium can be described by a multinomial distribution of processes in which a multiple charge is transferred. More importantly, we have shown that the calculation of the FCS allows us to identify the probability of the individual MARs and the charge transferred in these processes. This information probably provides the deepest insight into the transport properties of these systems. In this sense, in this work we present a comprehensive analysis of the dc transport properties of superconducting point contacts from the point of view of the FCS. We shall show that even in the most well-studied situations the FCS provides a fresh view. Moreover, we show that the FCS allows a unified description of many different type contacts. We also extend the analysis presented in Ref. [34] to finite temperature.

The paper is organized as follows. In section II, after introducing some basic concepts of charge statistics, we discuss the calculation of the cumulant generating functional within the Keldysh-Green's function approach. Section III is devoted to the calculation of the MAR probabilities at zero temperature. We present both the results of a toy model and the full expressions. In section IV we apply the results of the previous section to describe the different transport properties of three different

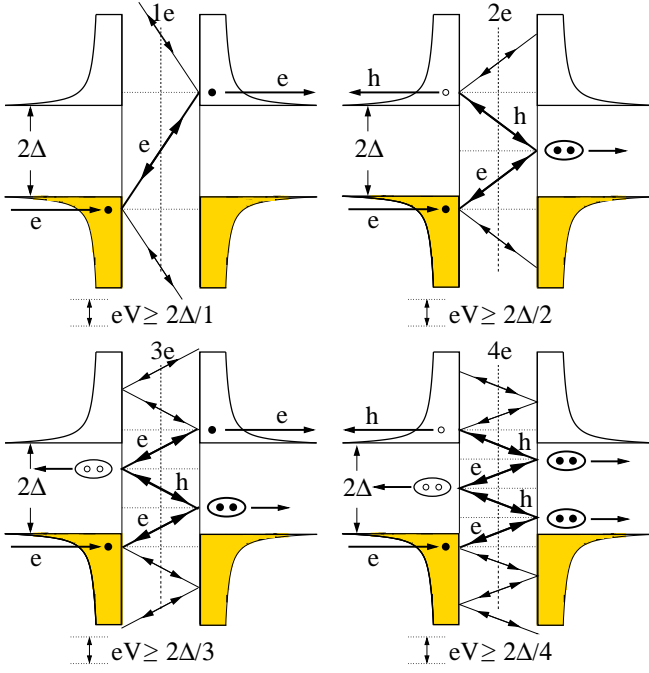


FIG. 1: Schematic representation of the MARs for BCS superconductors with gap Δ . We have sketched the density of states of both electrodes. In the upper left panel we describe the process in which a single electron tunnels through the system overcoming the gap due to a voltage $eV \geq 2\Delta$. The other panels show MARs of order $n = 2; 3; 4$. In these processes an incoming electron at energy E undergoes at least $n - 1$ Andreev reflections to finally reach an empty state at energy $E + neV$. In these MARs a charge ne is transferred with a probability, which for low transparencies goes as T^n . At zero temperature they have a threshold voltage $eV = 2\Delta/n$. The arrows pointing to the left in the energy trajectories indicate that a quasiparticle can be normally reflected. The lines at energies below E and above $E + neV$ indicate that after a detour a quasiparticle can be backscattered to finally contribute to the MAR of order n .

situations: (i) a contact between BCS superconductors, (ii) a contact between superconductor with a modified density of states due to a pair-breaking mechanism, and (iii) a short disusive SNS contact. In section V we analyze the transport at finite temperature paying special attention to the third cumulant. Finally, we present our conclusions in section VI.

II. DESCRIPTION OF THE FORMALISM

A. Some basic concepts

Our goal is to calculate the full counting statistics of a superconducting contact. This means that the quantity that we are interested in is the probability $P_{t_0}(N)$, that N charges are transferred through the contact in the time interval t_0 . Equivalently, we can find the cumulant generating function (CGF) $S_{t_0}(\chi)$, which is simply the

logarithm of the characteristic function and is defined by

$$\exp(S_{t_0}(\chi)) = \sum_N P_{t_0}(N) \exp(iN\chi) : \quad (1)$$

Here, χ is the so-called counting field. From the knowledge of the CGF one easily obtains the different cumulants that characterize the probability distribution

$$C_n = (-i)^n \frac{\partial^n}{\partial \chi^n} S_{t_0}(\chi) \Big|_{\chi=0} : \quad (2)$$

Notice that the first cumulants are related to the moments of the distribution as follows

$$C_1 = \overline{N} = \sum_N N P_{t_0}(N) ; C_2 = \overline{N^2} - \overline{N}^2 ; \\ C_3 = \overline{N^3} - 3\overline{N}\overline{N^2} ; C_4 = \overline{N^4} - 3C_2^2 ; \quad (3)$$

and so on. It is also important to remark that these cumulants have a simple relation with the relevant transport properties that are actually measured. Thus, for instance, the mean current is given by $I = (e/t_0)C_1$ and the symmetrized zero frequency noise is given by $S_I = (2e^2/t_0)C_2$ [75]. For higher cumulants such relations are not straightforwardly obtained, but it can be shown that the cumulants defined above correspond to the observable quantities in an electron counting experiment [47, 60, 61]. Thus, the cumulants represent all information, which is available in a measurement of the charge accumulated during the observation period t_0 .

B. Keldysh-Green's function approach to FCS

As mentioned above, our system of interest is a voltage-biased superconducting point contact, i.e. two superconducting electrodes linked by a constriction, which is much shorter than the superconducting coherence length. We concentrate ourselves on the case of a single channel contact described by a transmission probability T . The main difficulty in the determination of the FCS arises from the ac-Josephson effect. Here, a constant applied bias voltage eV gives rise to time-dependent currents as a consequence of the Josephson relation $(\partial/\partial t)\varphi(t) = 2eV/\hbar$. In the long-time limit $t_0 \gg \hbar/eV$ these oscillating currents do not contribute to the net charge transfer, in which we are interested. However, this intrinsic time-dependence is reflected in the CGF and a little care has to be taken, when the FCS is defined.

To obtain the FCS in a superconducting point contact we make use of the Keldysh-Green's function approach to FCS introduced by Nazarov and one of the authors [41, 47], and we refer to reader to these papers for further details on the basis of this theoretical approach. In what follows, we concentrate ourselves on the specific difficulties introduced in the case of a contact between two superconductors. Our starting point for the

determination of the CGF is to define the relation between the CGF and the counting current in analogy to Refs. [41, 47]:

$$\frac{\partial}{\partial t_0} S_{t_0}(\epsilon) = \frac{i}{e} \int_0^{t_0} dt I(\epsilon; t) : \quad (4)$$

This scalar current can be calculated in terms of the matrix current which describes the transport properties of the contacts. Nazarov has shown that, in the case of short junctions the matrix current (in Keldysh-Nambu space) adopts the following form [63]

$$I(\epsilon; t; t^0) = \frac{e^2}{4 + T} \frac{2T}{fG_1(\epsilon); G_2} \frac{G_1(\epsilon); G_2}{2} (t; t^0) : \quad (5)$$

Here $G_{1(2)}(t; t^0)$ denote the matrix Green's functions on the left and the right of the contact. In our problem these functions depend on two time arguments and the products appearing in Eq. (5) should be understood as convolutions over the intermediate time arguments, i.e. $(A \otimes B)(t; t^0) = \int dt^0 A(t; t^0) B(t^0; t^0)$. It is worthwhile to note, that the derivation for the matrix current in Ref. [63] was done for Green's functions in the static situation, in which case all Green's functions depend only on $t - t^0$. However, the derivation can be directly taken over to time-dependent problems, because the time-dependent Green's functions satisfy the normalization condition

$$(G \otimes G)(t; t^0) = \delta(t - t^0) : \quad (6)$$

Finally, the time-dependent scalar current is obtained from the matrix current by

$$I(\epsilon; t) = \frac{1}{4e} \text{Tr}_K I(\epsilon; t; t) : \quad (7)$$

where $K = \hat{\tau}_3$ is a matrix in Keldysh(Nambu) space. $\hat{\tau}_i(i)$ are the standard Pauli matrices in Keldysh(Nambu)-space.

Let us now describe Green's functions entering Eq. (5). The counting field is incorporated into the matrix Green's function of the left electrode as follows

$$G_1(\epsilon; t; t^0) = e^{i\epsilon t} G_1(t; t^0) e^{-i\epsilon t^0} : \quad (8)$$

Here $G_1(t; t^0)$ is the reservoir Green's function in the absence of the counting field. We set the chemical potential of the right electrode to zero and represent the Green's functions by

$$G_1(t; t^0) = e^{i(t-t^0)\phi/2} G_S(t - t^0) e^{-i(t-t^0)\phi/2} \quad (9)$$

and $G_2(t; t^0) = G_S(t - t^0)$. Here, $\phi(t) = \phi_0 + (2eV/\hbar)t$ is the time-dependent superconducting phase difference, and ϕ_0 is its dc part. G_S is the Green's function of a

superconducting reservoir (we consider the case of a symmetric junction), which reads

$$G_S(t - t^0) = \int_{-\infty}^{\infty} dE G_S(E) e^{iE(t - t^0)} ; \quad (10)$$

$$G_S(E) = \frac{(A - R)f + R}{(A - R)(1 - f) - R} \frac{(A - R)f}{R(A)f + A} :$$

Here, $R(A)(E)$ are retarded and advanced Green's functions of the leads and $f(E)$ is the Fermi function. Advanced and retarded functions in (10) have the Nambu-structure $R(A) = g^{R,A}_3 + f^{R,A}_1$ fulfilling the normalization condition $f^2 + g^2 = 1$. They depend on energy and the superconducting order parameter.

Using the time dependence of the leads Green's functions it is easy to show from Eq. (5) that the scalar current admits the following Fourier series

$$I(\epsilon; t) = \sum_n I_n(\epsilon) e^{in\phi(t)} ; \quad (11)$$

which means that the current oscillates with all the harmonics of the Josephson frequency. It is important to stress that the components $I_n(\epsilon)$ are independent of dc part of the superconducting phase. In this work we only want to consider the dc part of the CGF. For this purpose, we take the limit of a long measuring time t_0 , much larger than the inverse of the Josephson frequency, and hereafter we drop the subindex t_0 in the expression of the CGF. From Eq. (4) and Eq. (11) it is obvious that by selecting the dc component, the dc part of the phase drops the calculation and the CGF is free of the problems related to gauge invariance found for the dc Josephson effect [47, 60, 64].

Keeping in mind the presence of the time integration described above, and with the help of Eqs. (5-7), one can integrate Eq. (4) to obtain the following expression for the CGF of superconducting constrictions [47]

$$S(\epsilon) = \frac{t_0}{h} \text{Tr} \ln [1 + \frac{T}{4} fG_1(\epsilon); G_2] : \quad (12)$$

The symbol Tr implies that the products of the Green's functions are convolutions over the internal energy arguments, i.e.

$$(G_1 \otimes G_2)(E; E^0) = \int_{-\infty}^{\infty} dE_1 G_1(E; E_1) G_2(E_1; E^0) : \quad (13)$$

The trace runs not only over the Keldysh-Nambu space, but also includes a trace in the energy arguments, i.e. $\int dE g(E; E)$.

The time-dependent Green's functions of Eq. (8) fulfill the normalization condition of Eq. (6). This enables us to use the relation

$$2 fG_1; G_2 g = G_1 - G_2^2 \quad (14)$$

to write the CGF as

$$S(\lambda) = \frac{t_0}{h} \text{Tr} \ln Q_+ + \ln Q_-; \quad (15)$$

where $Q_{\pm} = 1 - \frac{p}{T} \frac{\partial}{\partial E} G_{\pm}(\lambda)$. One can show that both logarithms give the same contribution, and therefore we concentrate in the analysis of the first one, and we drop the subindex $+$. Additionally, we use the relation $\text{Tr} \ln Q = \ln \det Q$ to write the CGF as

$$S(\lambda) = \frac{t_0}{h} \ln \det Q(\lambda); \quad (16)$$

Thus, at this stage the calculation reduces to the calculation of the determinant of a infinite matrix. Due to the time dependence of the lead Green's functions their form in energy space is $G(E; E^0) = \sum_n G_{0,n}(E)(E - E^0 + n\epsilon)^{-1}$, where $n = 0; \pm 2$. This implies that the matrix Q also admits the same type of representation, which

in practice means that Q is a block-tridiagonal matrix of the form

$$Q = \begin{pmatrix} 0 & & & & & & 1 \\ & \ddots & & & & & \\ & & Q_{2;4} & Q_{2;2} & Q_{2;0} & 0 & \\ & & 0 & Q_{2;0} & Q_{0;0} & Q_{0;2} & 0 \\ & & & 0 & Q_{2;0} & Q_{2;2} & Q_{2;4} \\ & & & & 0 & \ddots & \ddots & \ddots \\ & & & & & & & 0 \end{pmatrix};$$

where we have used the notation $Q_{n,m} = Q(E + n\epsilon; E + m\epsilon)$. The different (4×4) matrices $Q_{n,m}$ have the following explicit form in terms of the advanced and retarded Green's functions $g^{R,A}$ and $f^{R,A}$ (remember that we consider a symmetric junction)

$$\begin{aligned} Q_{n,n} &= 1 + \frac{p}{2} \frac{\partial}{\partial E} \begin{pmatrix} 0 & n+1 & n+g_{n+1}^R & g_n^R \\ & \tilde{n} & f_n^R & \tilde{n} \\ & e^{i\tilde{n}+1} & n & \\ & \tilde{n} & e^{i\tilde{n}+1+n} & n \\ & 0 & 0 & 0 \end{pmatrix} \\ Q_{n,n+2} &= \frac{p}{2} \frac{\partial}{\partial E} \begin{pmatrix} 0 & 0 & e^{i(\tilde{n}+1+f_{n+1}^R)} & 0 \\ & 0 & 0 & \tilde{n}+1 \\ & 0 & \tilde{n}+1 & 0 \\ & 0 & 0 & 0 \end{pmatrix} \\ Q_{n,n-2} &= \frac{p}{2} \frac{\partial}{\partial E} \begin{pmatrix} 0 & 0 & 0 & 0 \\ & e^{i(\tilde{n}-1+f_{n-1}^R)} & 0 & \tilde{n}-1 \\ & 0 & 0 & 0 \\ & \tilde{n}-1 & 0 & e^{i(f_{n-1}^A)} \end{pmatrix} \end{aligned} \quad (17)$$

where we have used the shorthand notation $g_n^{R,A} = g^{R,A}(E + n\epsilon)$, $f_n = (g_n^A - g_n^R)f$, $\tilde{n} = (f_n^A - f_n^R)f$, $\tilde{n} = (g_n^A - g_n^R)(1 - f)$, and $\tilde{n} = (f_n^A - f_n^R)(1 - f)$.

One can restrict the fundamental energy interval to $E \in [E^0 - 2\epsilon; E^0 + 2\epsilon]$, and therefore the CGF adopts the form $S(\lambda) = (t_0/h) \int_{-2\epsilon}^{2\epsilon} dE \ln \det Q$. From Eq. (17), it is obvious that $\det Q$ can be written as the following Fourier series in

$$\det Q(\lambda) = \sum_{n=-\infty}^{\infty} P_n^0(E; V) e^{in\lambda}; \quad (18)$$

where the coefficients $P_n^0(E; V)$ have still to be determined. Keeping in mind the normalization $S(0) = 0$, it is clear that one can rewrite the CGF in the following form

$$S(\lambda) = \frac{t_0}{h} \int_{-2\epsilon}^{2\epsilon} dE \ln \left(1 + \sum_{n=1}^{\infty} P_n(E; V) e^{in\lambda} \right); \quad (19)$$

where

$$P_n(E; V) = P_n^0(E; V) = \sum_{n=-\infty}^{\infty} P_n^0(E; V); \quad (20)$$

Eq. (19) has the form of the CGF of a multinomial distribution in energy space (provided more than one P_n is different from zero). The different terms in the sum in Eq. (19) correspond to transfers of multiple charge quanta at energy E with the probability $P_n(E; V)$, which can be seen by the $(2\pi n)$ -periodicity of the accompanying λ -dependent counting factor. This is the

main result of our work and it proves, that the charges are indeed transferred in large quanta. Of course, we still have to determine the probabilities $P_n(E; V)$, which is a non-trivial task and it will be the goal of the next section.

C. Cumulants

As explained before, from the CGF one can easily calculate the cumulants of the distribution and in turn many

transport properties. Of special interest are the first three cumulants C_1, C_2 and C_3 , which correspond to the average, width and skewness of the distribution of transmitted charge, respectively. From Eq. (2) and Eq. (19), it follows that these cumulants can be expressed in terms of the probabilities $P_n(E; V)$ as follows

$$C_1 = \frac{t_0}{h} \int_0^{eV} dE \sum_n n P_n; \quad (21)$$

$$C_2 = \frac{t_0}{h} \int_0^{eV} dE \sum_n n^2 P_n - \left(\sum_n n P_n \right)^2; \quad (22)$$

$$C_3 = \frac{t_0}{h} \int_0^{eV} dE \sum_n n^3 P_n - 3 \sum_n n P_n \sum_n n^2 P_n + 2 \left(\sum_n n P_n \right)^3; \quad (23)$$

These expressions are a simple consequence of the fact that the charge transfer distribution is multinomial in energy space. At zero temperature the sums over n are restricted to positive values ($n \geq 1$). We remind the reader that the first two cumulants are simply related to the dc current, $I = (e/t_0)C_1$, and to the zero-frequency noise $S_I = (2e^2/t_0)C_2$.

It is instructive to discuss some consequences of these expressions. Let us first recall, what happens when only one process contributes, which has, e.g., the order n . The first three cumulants are

$$C_{1,n} = n \int_0^{eV} \frac{t_0 dE}{h} P_n; \quad (24)$$

$$C_{2,n} = n^2 \int_0^{eV} \frac{t_0 dE}{h} P_n (1 - P_n); \quad (25)$$

$$C_{3,n} = n^3 \int_0^{eV} \frac{t_0 dE}{h} P_n (1 - P_n) (1 - 2P_n); \quad (26)$$

We see, that the i^{th} cumulant is proportional n^i , i.e. the i^{th} power of the charge of the respective elementary event. The expressions under the integral in Eqs. (24-26) have the same form as for binomial statistics, however in

general the $P_n(E; V)$ depend on energy in a nontrivial way and the energy-integrated expressions for the cumulants do not correspond to binomial statistics. A simple interpretation in terms of an effective charge transferred is only possible if $P_n(E; V) = 1$ for all energies, in which case one recovers the standard result for Poisson statistics, $C_{i,n} = n^{i-1} C_{1,n}$. According to Eq. (26) the sign of the spectral third cumulant can be positive or negative, depending on the size of P_n (positive for $P_n < 1/2$ and negative for $P_n > 1/2$). The overall sign depends on the energy average and is not simple to predict. Note, however, that the probabilities of MAR-processes of higher orders decrease approximately as T^n . We may therefore speculate that to obtain a negative third cumulant for higher order processes we will need more open contacts (a rough estimate is thus that $T \lesssim 1/2$ to have $P_n \approx 1/2$ and, therefore, $C_3 < 0$).

The general statistics (19) is a multinomial distribution and it is therefore interesting to compare with independent binomial distributions. This is most easily done by assuming, that only two processes compete. Taking these processes to be of order n and m the first three cumulants read

$$C_{1nm} = C_{1n} + C_{1m} ; \quad (27)$$

$$C_{2nm} = C_{2n} + C_{2m} - 2nm \int_{-Z_0}^{Z_0} \frac{t_0 dE}{h} P_n P_m ; \quad (28)$$

$$C_{3nm} = C_{3n} + C_{3m} - 3nm \int_0^{Z_0} \frac{t_0 dE}{h} P_n P_m [n(1 - P_n) + m(1 - P_m)] : \quad (29)$$

We see that the first cumulant is just the sum of the contributions of the different processes n and m and we therefore have to look at higher cumulants to gain information on correlations between the processes of different order. In both, the second and the third cumulant, such correlations appear and it is evident from Eqs. (28) and (29) that both are reduced below the value obtained for independent binomials. The correlation terms appear inside the energy integration and therefore both processes must be possible at the same energy.

Finally, we note that in order to study correlation between N different processes one would have to look at the N th order cumulant. This becomes clear if one notices that only the N th cumulant contains a term with products of N probabilities and therefore the possibility to have a product of probabilities of N different processes.

III. MAJOR PROBABILITIES: ZERO TEMPERATURE

This section is devoted to the calculation of the probabilities $P_n(E; V)$ at zero temperature. First, we discuss a simple model which nicely illustrates the transmission dependence of these probabilities, and secondly we present the general expressions.

A. Toy model

To obtain a feeling for the forthcoming calculations we will now study a strongly simplified model of a superconducting contact. For that purpose, let us assume that we can neglect the Andreev reflections for energies outside the gap region and replace the quasiparticle density of states by a constant for $E > \Delta$. Furthermore, we neglect that energy-dependent phase shift $\phi(E) = \arccos(E/\Delta)$, usually associated with the finite penetration of excitations close to the gap edge. Mathematically, this means that we set $f^{R(A)}(E < \Delta) = 1$, $g^{R(A)}(E > \Delta) = 1$, and both are equal to zero otherwise. This simplifies the calculation a lot, since the matrix Q in Eq. (16) now becomes finite. In particular, for subharmonic voltage $eV = 2\Delta$ the matrix is also energy-independent. It is interesting to note that the toy model is also able to describe the counting statistics of normal contacts and Andreev contacts.

super:	$E > \Delta$	$ j\rangle \langle j E > \Delta$	$E > \Delta$
normal:	$E > eV$		$E < eV$
$\hat{g}_{11}(\epsilon)$	$\hat{K}^-(\epsilon)$	0	$\hat{K}^+(\epsilon)$
$\hat{g}_{22}(\epsilon)$	$\hat{K}^-(\epsilon)$	0	$\hat{K}^+(\epsilon)$
$\hat{g}_{12(21)}(\epsilon)$	0	$e^{i\phi}$	0

TABLE I: Green's functions in the toy model. The indices \hat{g} denote the respective element in Nambu space. $\hat{K}^\pm = \hat{\tau}_3 \hat{2}^{\pm} e^{i\phi}$ denotes a matrix in Keldysh space. The table holds for left and right terminal, provided the energies and the counting fields are chosen properly.

To facilitate the discussion of the matrix structure it is useful to introduce the 2×2 matrix in the Keldysh sub-space

$$\hat{K}^\pm(\epsilon) = \hat{\tau}_3 \hat{2}^{\pm} e^{i\phi} ; \quad (30)$$

where $\hat{\tau}_i$ are Pauli matrices and $\hat{2}^\pm = (\hat{\tau}_1 \pm i\hat{\tau}_2)/2$. In fact, \hat{K}^\pm correspond to occupied (empty) quasiparticle states (for $E > \Delta$). The matrix structure for superconducting or normal terminals is summarized in Table I. The counting statistics is obtained from the general relation (16)

$$S(\epsilon; V) = \frac{2t_0}{h} \int_0^{Z_0} dE \text{Tr} \ln \left[1 + \frac{p}{2} \frac{1}{T} G_1(\epsilon) G_2(\epsilon) \right] ; \quad (31)$$

The incorporation of the energy discretization is obtained by a redefinition of the trace in the above formulas, and a limitation of the energy integration to an interval of width eV . Note, that we have to evaluate only one of the two terms $\frac{p}{2} \frac{1}{T}$, since the FCS can only depend on T and not on $\frac{p}{2} \frac{1}{T}$.

To calculate the determinant we note that Q is a band matrix of width 3 in the energy index. Then the following reduction formula for the determinant is useful (assuming

a block starts at some n , which we arbitrarily set to zero):

$$\begin{pmatrix}
 Q_{0;0} & Q_{0;2} & 0 & 0 \\
 Q_{2;0} & Q_{2;2} & Q_{2;4} & 0 \\
 0 & Q_{4;2} & Q_{4;4} & \ddots \\
 0 & 0 & \ddots & \ddots
 \end{pmatrix} = \begin{pmatrix}
 Q_{2;2} & Q_{2;0}Q_{0;2} & Q_{2;4} & 0 \\
 Q_{0;0} & Q_{4;2} & Q_{4;4} & \ddots \\
 0 & \ddots & \ddots & \ddots
 \end{pmatrix} \quad (32)$$

Another useful property (which holds in the toy model) is the Nambu structure of the Q 's, see Eq. (17) and Table I: diagonal components in energy space, i.e. $Q_{n;n}$, are always block-diagonal in Nambu space and the off-diagonal components $Q_{n;n \pm 2}$ are purely off-diagonal in Nambu space and diagonal in Keldysh-space. Consequently, $Q_{n \pm 2;n \pm 2} = Q_{n \pm 2;n} Q_{n;n \pm 2}^{-1} Q_{n;n \pm 2}$ appearing in the expansion of the determinant is block-diagonal again and the whole calculation of the determinant (16) boils down to a recursive calculation of determinants and inversions of 2×2 -matrices. This will become more clear, when we will treat the explicit examples below.

1. Normal Contact

It is instructive to demonstrate the procedure first for a normal contact. The Green's functions are (we restrict the calculation here to electron block, the hole block gives actually the same contribution)

$$\hat{G}_1 = \begin{pmatrix} \hat{K}^- & 0 \\ \hat{K}_+ & 0 \end{pmatrix}; \hat{G}_2 = \begin{pmatrix} \hat{K}^-(0) & 0 \\ \hat{K}_+(0) & 0 \end{pmatrix}; \quad (33)$$

Note that we have chosen the fundamental energy interval $[-eV/2; eV/2]$, since then the Green's functions are constant inside each interval. Then we find

$$\frac{(\hat{Q}^{-1})_{h,m}}{T=2} = \begin{matrix} 8 \\ < \hat{+} (e^i - 1) & n > 0 \\ & \hat{+}_3 + \hat{+}_+ e^i & n = 0 \\ : & \hat{+} (e^{-i} - 1) & n < 0 \end{matrix} \quad (34)$$

The matrix Q has thus block diagonal form. The blocks $n > 0$ and $n < 0$ are tridiagonal and the determinants are all equal to 1. The remaining determinant of the $n = 0$ block is

$$\det \left(1 + \frac{p}{T} \frac{p}{T} \frac{p}{T} \frac{p}{T} \right) = 1 - T + T e^i \quad (35)$$

The CGF is finally $S(\epsilon) = (2eV t_0 / h) \ln(1 + T(e^i - 1))$ in agreement with Levitov and Lesovik [37]. Notice that a factor of 2 enters the CGF, because we get an additional contribution from the hole block (thus it is due to spin).

2. Andreev contact

We now consider a contact in which one of the sides is superconducting and the other is a normal metal. Again, the calculation can be done in a similar way. Here we apply a voltage ϵV to the normal contact. The Green's functions are again diagonal in the energy space, since we assume that the superconductor is at zero potential. For the normal metal we find (taking as fundamental energy interval $[-eV/2; eV/2]$)

$$\hat{G}_1 = \begin{pmatrix} \hat{K}^- & 0 \\ \hat{K}_+ & 0 \end{pmatrix}; \hat{G}_2 = \begin{pmatrix} \hat{K}^- & 0 \\ \hat{K}_+ & 0 \end{pmatrix}; \quad (36)$$

and for the superconductor $\hat{G}_2 = \hat{G}_2 = \hat{G}_1$ and 0 otherwise. The only non-zero block is the $n = 0$ energy block

$$G_1(\epsilon) G_2 = \begin{pmatrix} K^- & 1 \\ 1 & K_+ \end{pmatrix}; \quad (37)$$

which yields for the CGF in the form (12) the determinant of

$$Q = \begin{pmatrix} 1 & \frac{T}{2} & \frac{T}{4} (\hat{K}_+ - \hat{K}^-) \\ \frac{T}{4} (\hat{K}_+ - \hat{K}^-) & 1 & \frac{T}{2} \end{pmatrix}; \quad (38)$$

To calculate the determinant we subtract from rows 3 and 4 the rows 1 and 2 multiplied with $\frac{T}{4}(1 - \frac{T}{2})(\hat{K}_+ - \hat{K}^-)$ and make use of the fact that $(\hat{K}^- - \hat{K}_+)^2 = 4(1 - e^{i2})$. The matrix is then tridiagonal and its determinant is

$$1 - \frac{T}{2} + 1 + \frac{T^2}{(2 - T)^2} e^{i2} = 1 \quad (39)$$

The prefactor is canceled because we are operating under the \ln and have to normalize. Notice that the evaluation of the determinant outside the transport window can be done in a similar way. One obtains for the determinant of one block $(1 - T/2)^2 - T^2 (\hat{K}^- - \hat{K}_+)^2 = (1 - T/2)^2$, which is independent of the counting field and is therefore canceled after normalization of the CGF. Finally we obtain for the FCS (collecting all prefactors) [48]

$$S(\epsilon) = \frac{2eV t_0}{h} \ln \left(1 + \frac{T^2}{(2 - T)^2} e^{i2} \right) \quad (40)$$

The statistics corresponds to a binomial distribution of charge transfers. The Andreev reflection leads to a π -periodicity in ϵ which shows that only couples of charges can be transferred and the charge transfer probability for odd charge numbers vanishes. The number of attempts, determined by the prefactor of the \ln in (40), remains unchanged in comparison to the normal case.

3. Superconducting point contact

We now come to the main subject of the article, a point contact between two superconducting banks held at different chemical potentials. To write down the general matrix structure of the FCS in the toy model, let us first obtain the condition for energies to be subgap. Here, we restrict ourselves to subharmonic voltages, which we write in general as $eV = 2 = (N - 1)$, where N denotes the order. The dominating charge transport mechanism we expect is that N charges are transferred. In the toy-model, it is the only transport mechanism (since Andreev reflections above the gap are neglected). To obtain a single-valued matrix entries, it is favourable to choose as fundamental energy interval $[0; eV]$ for even $N = 2M$ and $[eV/2; eV/2]$ for odd $N = 2M + 1$. For the Nambu row indices of the Green's function of the left terminal we find

Nambu	Order	E_j
upper	odd	$M - n \quad M - 1$
lower	odd	$M + 1 \quad n \quad M$
upper	even	$M - 1 \quad n \quad M - 1$
lower	even	$M \quad n \quad M$

(41)

The row indices in Nambu space of the right Green's functions have the energy arguments of upper and lower row interchanged.

To clarify the matrix structure we have prepared a small table. Each entry denotes the energy for the structure $\frac{g_{1i}^L}{g_{2i}^L} | \frac{g_{1i}^R}{g_{2i}^R}$, where the second (Nambu-) index $i = 1; 2$ plays no role. The entries are denoted by + for $E > 0$, 0 for $E_j = 0$, and - for $E < 0$.

n	$N = 2$	$N = 3$	$N = 4$	$N = 5$	$N = 6$
2	$\begin{matrix} + & + \\ + & + \end{matrix}$	$\begin{matrix} + & + \\ + & + \end{matrix}$	$\begin{matrix} + & + \\ + & + \end{matrix}$	$\begin{matrix} + & 0 \\ 0 & + \end{matrix}$	$\begin{matrix} + & 0 \\ 0 & + \end{matrix}$
1	$\begin{matrix} + & + \\ + & + \end{matrix}$	$\begin{matrix} + & 0 \\ 0 & + \end{matrix}$	$\begin{matrix} + & 0 \\ 0 & + \end{matrix}$	$\begin{matrix} 0 & 0 \\ 0 & 0 \end{matrix}$	$\begin{matrix} 0 & 0 \\ 0 & 0 \end{matrix}$
0	$\begin{matrix} + & 0 \\ 0 & + \end{matrix}$	$\begin{matrix} 0 & 0 \\ 0 & 0 \end{matrix}$	$\begin{matrix} 0 & 0 \\ 0 & 0 \end{matrix}$	$\begin{matrix} 0 & 0 \\ 0 & 0 \end{matrix}$	$\begin{matrix} 0 & 0 \\ 0 & 0 \end{matrix}$
1	$\begin{matrix} 0 \\ 0 \end{matrix}$	$\begin{matrix} 0 \\ 0 \end{matrix}$	$\begin{matrix} 0 & 0 \\ 0 & 0 \end{matrix}$	$\begin{matrix} 0 & 0 \\ 0 & 0 \end{matrix}$	$\begin{matrix} 0 & 0 \\ 0 & 0 \end{matrix}$
2			$\begin{matrix} 0 \\ 0 \end{matrix}$	$\begin{matrix} 0 \\ 0 \end{matrix}$	$\begin{matrix} 0 & 0 \\ 0 & 0 \end{matrix}$
3					$\begin{matrix} 0 \\ 0 \end{matrix}$

(42)

We observe that the matrix structure in all cases is similar. A block with 0 and + elements, i.e. connecting the quasiparticle states above the gap to the subgap region is followed a number of blocks inside the gap (depending on the applied voltage and, finally, is connected by a block with 0 and - elements to quasiparticle states below the gap.

Let us now discuss the case $N = 2$ ($eV = 2$). Here

the relevant 8 × 8-matrix is

$$\frac{Q}{T=2} = \begin{pmatrix} 0 & \hat{K}^- & 0 & 0 & 1 & 1 \\ 0 & \hat{K}^-(0) & e^{i\phi_3} & 0 & 0 & 0 \\ 0 & e^{i\phi_3} & \hat{K}^+(0) & 0 & 0 & 0 \\ 1 & 0 & 0 & \hat{K}^+ & 0 & 0 \end{pmatrix} \quad (43)$$

We observe, that the matrix decouples into two blocks of 4 × 4 matrices

$$Q_{2A} = 1 + \frac{P}{T} \begin{pmatrix} \hat{K}^- & 1 \\ 1 & \hat{K}^+ \end{pmatrix} \quad (44)$$

and

$$Q_{2B} = 1 + \frac{P}{T} \begin{pmatrix} \hat{K}^-(0) & e^{i\phi_3} \\ e^{i\phi_3} & \hat{K}^+(0) \end{pmatrix} : \quad (45)$$

By comparison with Eq. (37) we see that $\ln \det Q_{2A}$ yields the counting statistics of usual Andreev reflection. Q_{2B} gives actually the same result. This is most easily seen, if the unitary transformation $U Q_{2B} U^\dagger$ with $U = \text{diag}(e^{i\phi_3/2}, e^{i\phi_3/2})$ is applied, which transforms Q_{2B} into Q_{2A} . Note, that the signs of the off-diagonal matrices do not matter, since they can be eliminated by similar unitary transformations. The counting statistics is therefore given by Eq. (40), the same as for the Andreev contact.

Now we come to the slightly more complicated case $N = 3$ ($eV = 2 = 2$). Here we encounter the matrix

$$\frac{Q}{T=3} = \begin{pmatrix} 0 & \hat{K}^- & 0 & 0 & 1 & 0 & 0 & 1 \\ 0 & \hat{K}^-(0) & e^{i\phi_3} & 0 & 0 & 0 & 0 & 0 \\ 0 & e^{i\phi_3} & 0 & 0 & 0 & 0 & 1 & 0 \\ 1 & 0 & 0 & 0 & e^{i\phi_3} & 0 & 0 & 0 \\ 0 & 0 & 0 & e^{i\phi_3} & \hat{K}^+(0) & 0 & 0 & 0 \\ 0 & 0 & 1 & 0 & 0 & \hat{K}^+ & 0 & 0 \end{pmatrix} : \quad (46)$$

Once again, the matrix decouples into two blocks (rows 1,4,5 and rows 2,3,6). The first block is

$$Q_{3A} = 1 + \frac{P}{T} \begin{pmatrix} \hat{K}^- & 1 & 0 & 1 \\ 1 & 0 & e^{i\phi_3} & 0 \\ 0 & e^{i\phi_3} & \hat{K}^+ & 0 \end{pmatrix} : \quad (47)$$

It is already evident, that we will encounter a three particle process, if we apply the transformation $U = \text{diag}(\exp(i\phi_3/3), \exp(i\phi_3/3), 1)$. This yields

$$U Q_{3A} U^\dagger = 1 + \frac{P}{T} \begin{pmatrix} \hat{K}^-(3) & 1 & 0 & 1 \\ 1 & 0 & 1 & 0 \\ 0 & 1 & \hat{K}^+ & 0 \end{pmatrix} : \quad (48)$$

Evaluating the determinant we obtain the counting statistics (including the other block, see below)

$$S(\epsilon) = \frac{2eV t_0}{h} \ln \left(1 + \frac{T^3}{(4 - 3T)^2} e^{i\phi_3} \right) : \quad (49)$$

Evidently this corresponds to the binomial transfer of packages of three charges, where the probability of a third order process is $P_3 = T^3 = (4 - 3T)^2$. A similar procedure may be applied to the second block Q_{3B} . The result is the same. Physically, the two blocks correspond to two independent processes which differ by the spin.

For higher order processes the calculation goes in complete analogy. The property of a decoupling into two independent blocks remains. Furthermore it is possible to shift the entire T -dependence to the uppermost (or the lowest) block. This is achieved by a series of unitary operations of the type $(1; \dots; 1; \exp(i\hat{\sigma}_3); 1; \dots; 1)$. One can easily convince oneself, that for a process of order N this gives e.g. the upper-left block $\hat{K}^-(N)$ and the remaining matrix is now independent of T . For example a 5th-order process yields

$$1 + \frac{P_5}{2} \begin{pmatrix} 0 & 1 \\ 1 & 0 \end{pmatrix} \hat{K}^-(5) \begin{pmatrix} 1 & 0 & 0 & 0 \\ 0 & 1 & 0 & 0 \\ 0 & 0 & 1 & 0 \\ 0 & 0 & 0 & 1 \end{pmatrix} \hat{K}^+(0) \begin{pmatrix} 0 \\ 1 \\ 0 \\ 0 \\ 1 \end{pmatrix} : \quad (50)$$

Additionally, the signs of the off-diagonal element may be removed by unitary transformations. Evaluating the determinant we find $S(\omega) = (2eV t_0 / \hbar) \ln [1 + P_5 e^{i\omega t_0}]$, where $P_5 = T^5 = (16 - 20T + 5T^2)^2$. This expression describes binomial transfers of 5 charges with probability P_5 .

Using the above scheme, it is also possible to derive recursion relations for the probabilities. We find the probability for a process of order N

$$P_N = \frac{1}{1 + \frac{P_{N-1}}{1 + \frac{P_{N-2}}{1 + \dots + \frac{P_1}{1 + \frac{P_0}{2}}}}} : \quad (51)$$

The factors $\frac{P_{N-1}}{1 + \dots}$ and $\frac{P_0}{2}$ are determined from the recursion relations

$$P_n = 1 - \frac{T}{4 - P_{n-1}} ; \quad P_n = \frac{T}{4 - P_{n-1} - P_{n-2}} ; \quad (52)$$

with the initial conditions

$$P_1 = \frac{P_0}{2} ; \quad P_1 = 1 - \frac{T}{2} : \quad (53)$$

For general subharmonic voltages $2 = (N - 1)$ we find the counting statistics

$$S(\omega) = \frac{2eV t_0}{\hbar} \ln [1 + P_N e^{i\omega t_0}] ; \quad (54)$$

where the probabilities are given by

$$P_2 = \frac{T^2}{(2 - T)^2} ; \quad (55)$$

$$P_3 = \frac{T^3}{(4 - 3T)^2} ;$$

$$P_4 = \frac{T^4}{(8 - 8T + T^2)^2} ;$$

$$P_5 = \frac{T^5}{(16 - 20T + 5T^2)^2} ;$$

$$P_6 = \frac{T^6}{(2 - T)^2 (16 - 16T + T^2)^2} ;$$

$$P_7 = \frac{T^7}{(64 - 112T + 56T^2 - 7T^3)^2} ;$$

Note the limiting cases of these probabilities $P_N = T^N = 4^{N-1}$ for $T = 1$ and $P_N = 1$ for $T = 1$.

We can draw several conclusions from the toy model. First we obtain simple expressions for the probabilities of multiple charge P_N , which are not simple products of Andreev reflection probabilities and quasiparticle transmissions, see Eq. (55). Furthermore it is interesting to note that by virtue of the unitary transformations we can interpret the charge transfer as simultaneous transmission of N quasiparticles. This explanation does not invoke any kind of combined transfer of Cooper pairs and quasiparticle.

B. Full expressions

Let us now discuss the full expression of the probabilities $P_n(E; V)$ at zero temperature. Since Q has a block-tridiagonal form, in order to calculate its determinant we can use the recursion technique similar to the one described for the toy model. We define the following 4×4 matrices

$$F_n = \begin{pmatrix} Q_{n+1,n} & Q_{n+1,n-1} & 2F_{n-2}^{-1} Q_{n-2,n} & n-2 \\ Q_{0,n} & Q_{0,n-1} & 2F_{-2}^{-1} Q_{-2,n} & Q_{0,2} F_2^{-1} Q_{2,n} \end{pmatrix} ; \quad (56)$$

With these definitions, $\det Q$ is simply given by $\det Q = \prod_{j=1}^N \det F_{2j}$. In practice, $\det F_n = 1$ if $n \neq j$. This reduces the problem to the calculation of the determinants of 4×4 matrices.

In the zero-temperature limit one can work out this idea analytically, and after very lengthy but straightforward algebra, we obtain the following expressions for $P_n^0(E; V)$

$$P_n(T=1) = \sum_{l=0}^{\infty} (1 - a_{n+1}^f) \sum_{k=n+1+l}^{\infty} a_k^f (1 - a_k^f); \quad (61)$$

where $a(E)$ is the Andreev reflection coefficient defined as $a(E) = \frac{1}{2} (1 + g^R(E))$, and $a_n = a(E + neV)$. As can be seen in Eq. (61), a quasiparticle can only move upwards in energy due to the absence of normal reflection. If we use this expression in the current formula we recover the result obtained by Klapper, Blonder and Tinkham [11] for $T = 1$.

IV. APPLICATION TO DIFFERENT SITUATIONS

As explained in the previous section, with the expression of the MAR probabilities we can easily describe many different transport properties. Moreover, notice that so far we have not made any assumption about the leads Green's functions $g^{A,R}$ and $f^{A,R}$ entering in the expressions of $P_n(E;V)$. Therefore, these expressions allow us to address a great variety of situations. In this section we analyze the zero-temperature transport properties of three different situations: (i) a contact between BCS superconductors, (ii) a contact between superconductor under the influence of pair-breaking mechanisms and (iii) a short disordered SNS contact, where N is a normal disordered region shorter than the superconducting coherence length.

A. BCS superconductors

Let us start analyzing the most standard situation, namely a contact between two BCS superconductors with a gap Δ . In this case $f^{A,R} = 0$ for $|E| < \Delta$, where $\Delta = 0^+$, and $g^{A,R}$ follows from normalization. As mentioned in the introduction the current and noise of such a contact have been thoroughly studied both theoretically [15, 16, 17, 18, 21, 22] and experimentally [28, 29, 30, 31, 32]. Our goal here is to show how the knowledge of the FCS provides a new and deeper insight into the different transport properties.

In Fig. 2 we show the first three cumulants of the charge transfer distribution: current, shot noise and skewness (third cumulant). Let us discuss their most remarkable features. (i) The current exhibits the so-called subharmonic gap structure, as discussed in the introduction. This subgap structure evolves from a step-like behavior for low transmission to its disappearance at perfect transparency. (ii) The shot noise in the subgap region can be much larger than the Poisson noise ($S_{I,Poisson} = 2eI$). Moreover, in the tunneling regime the effective charge defined as the ratio $q = S_I/2I$ is quantized in units of the electron charge: $q(V) = e =$

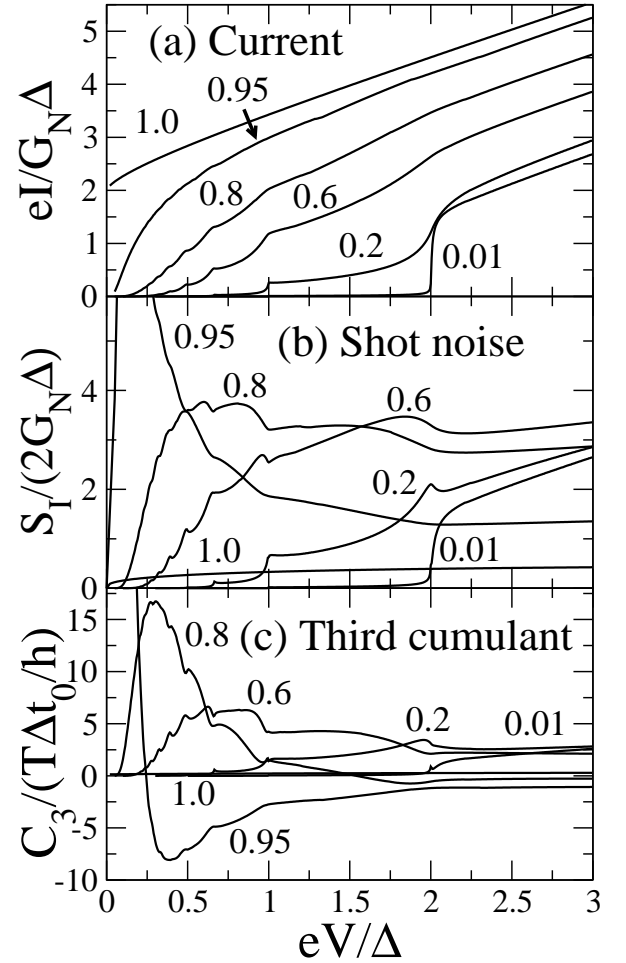


FIG. 2: Current, shot noise and third cumulant at zero temperature as a function of the voltage for BCS superconductors of gap Δ . The different curves correspond to different transmission coefficients as indicated in the panels. Here, $G_N = (2e^2/h)T$ is the normal state conductance.

$1 + \text{Int}(2\Delta/eV)$. This is illustrated in Fig. 3, where the ratios C_2/C_1 and C_3/C_1 are shown as a function of the voltage. (iii) As shown in Fig. 3, the third cumulant at low transmissions is described by $C_3 = q^2 C_1$, where again q is the quantized effective charge defined above. For higher transmissions this cumulant is negative at high voltage as in the normal state, where $C_3 = (t_0/h)T(1-T)(1-2T)eV$, but it becomes positive at low bias, and after this sign change there is a huge increase of the ratio C_3/C_1 .

The features described in the previous paragraph can be easily understood with the help of an analysis of the probabilities $P_n(E;V)$. To give an idea about them, in Fig. 4 we have plotted their average value defined as $P_n(V) = \int_0^{eV} dE P_n(E;V)$ for two very different transmissions. First of all, notice that, no matter what the transmission is, the probability of an n -order MAR has a threshold voltage $eV_n = 2\Delta/n$, below which the process is forbidden. When $V > V_n$ an n -order MAR

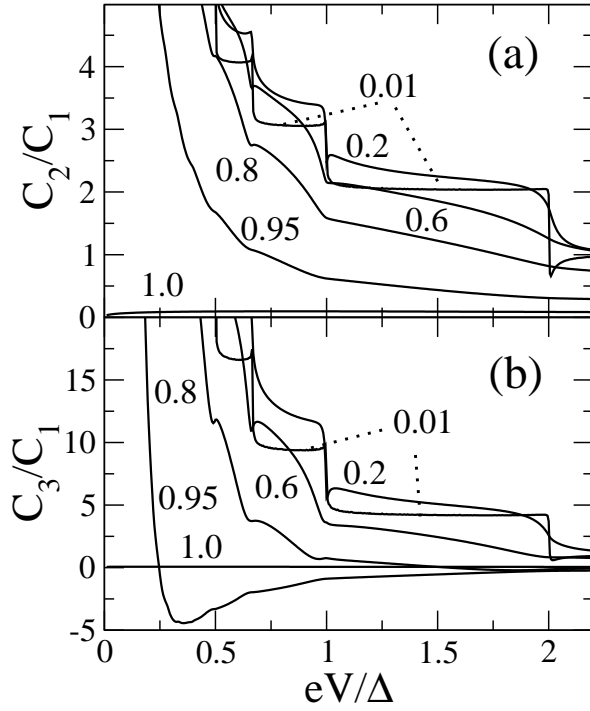


FIG. 3: (a) Second cumulant and (b) third cumulant at zero temperature for BCS superconductors. Both are normalized to the first cumulant (the average current). The transmissions are indicated in the plots.

gives a new contribution to the transport, which is usually the explanation of the subharmonic gap structure. On the other hand, the big difference between the tunneling regime and perfect transparency can be explained as follows. At low transparency there are two factors that make the subgap structure so pronounced. First, at V_n the n -order MAR is a process that connects the two gap edges, where the BCS density of states diverges (see Eq. (60)). This fact, together of course with its higher probability, implies that this MAR rapidly dominates the shape of the I-V curves giving rise to a non-linearity at V_n . Second, at V_n there is a huge enhancement of the probabilities of the MARs of order $m > n$. This is due to the fact that precisely at V_n the MAR trajectories can connect both gap edges, which as can be seen in Eq. (60) increases enormously their probability. At perfect transparency, the MAR probabilities do not exhibit any abrupt feature (see Fig. 4b). This is due to the fact that the BCS density of states is renormalized, and in particular, the divergences disappear (see Eq. (61)). This fact explains naturally why the subharmonic gap structure is completely washed out at $T = 1$.

Another interesting feature of the MAR probabilities occurs at low transparencies. As one can see in Fig. 4a, at a voltage $2 = n < eV < 2 = (n - 1)$ the MAR of order n has a much higher probability than the other MARs. This means that in this voltage window the n -order MAR clearly dominates the transport properties and the charge

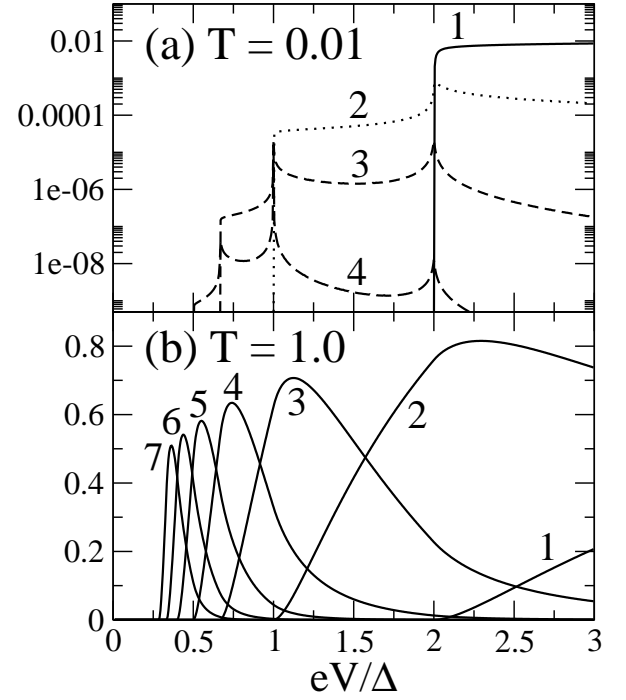


FIG. 4: Average MAR probabilities $P_n(V)$ ($1 = eV$) $\int_0^{eV} dE P_n(E; V)$ as a function of voltage for a contact between BCS superconductors at zero temperature. The two panels correspond to two different transmissions. The index of the processes is indicated in the plots. Notice the logarithmic scale in the panel (a).

is predominantly transferred in packets of ne . This fact explains the charge quantization in the tunneling regime observed both in C_2 and C_3 (see Fig. 3). More generally, this fact implies that at low transparencies the multinomial distribution of Eq. (19) becomes Poissonian, and in this limit all the cumulants are proportional to the current: $C_n = (q(V) = e)^n C_1$, where $q(V)$ is the voltage-dependent quantized charge. When the transmission is not very low, there are always several MARs that give a significant contribution to the transport at every voltage (see Fig. 4b). This explains why the charge is in general not quantized.

The explanation for the sign change of C_3 at low bias and high transparencies can be found in Eq. (23). In order to get a positive value for C_3 , one needs the first two terms in Eq. (23) to dominate, which happens when $P_n \approx 1$. This is precisely what happens at low bias, where the MAR probabilities are rather small. On the other hand, the huge enhancement after the sign change is due to the fact that n , the charge transferred by these MARs, is indeed huge at low bias.

Finally, at $T = 1$ the cumulants C_n (with $n > 1$) do not completely vanish due to the fact that at a given voltage different MARs give a significant contribution, and therefore their probability is smaller than one (see Fig. 4(b)).

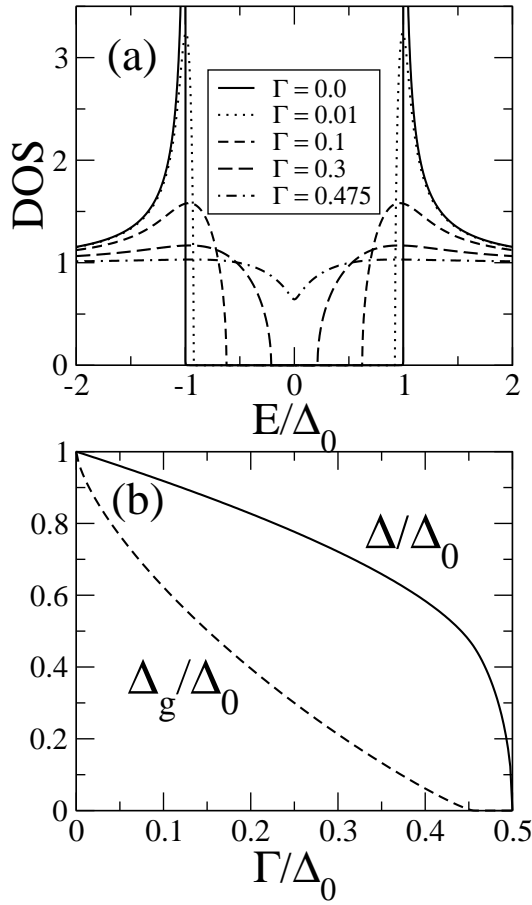


FIG. 5: (a) Density of states as a function of energy of a superconductor for different values of the depairing energy measured in units of gap in the absence of pair-breaking Δ_0 . (b) Order parameter and spectral gap Δ_g in units of Δ_0 as a function of the depairing energy normalized by Δ_0 .

B. Pair-breaking mechanisms

It is well-known that there are many mechanisms that can lead to pair-breaking effects, which modify the quasi-particle spectrum of a superconductor. Typical examples are a magnetic field, supercurrents or magnetic impurities. It was shown in the 1960's that for disordered superconductors various pair-breaking mechanisms can be described in a unified manner with a single parameter Γ , the depairing energy, which describes the strength of the pair-breaking [65]. The only difference between these mechanisms is contained in the microscopic expression of Γ . For instance, for thin film of thickness d much smaller than the superconducting coherence length in a magnetic field H parallel to the film $\Gamma = D e^2 d^2 H^2 / (6 \sim c^2)$, where D is the diffusion constant. In these situations the energy-dependent retarded Green's function can be calculated from [65]

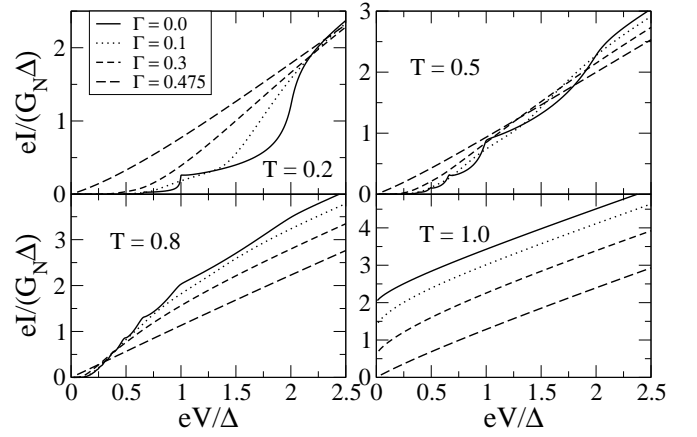


FIG. 6: Zero temperature current-voltage characteristics for superconductors with a depairing energy in units of Δ_0 . The current and the voltage have been normalized with the order parameter at the corresponding Γ . The different panels correspond to different transmissions values.

$$g^R = \frac{u}{u^2 - 1} = u f^R; \quad \frac{E}{u} = u \left(1 - \frac{1}{u^2} \right) \quad (62)$$

Here, u is the order parameter, which is in this case differs from the spectral gap and it has to be determined self-consistently [66]. For small Γ the pair-breaking mechanisms result in a smearing of the BCS singularities in the density of states and in a suppression of the spectral energy gap Δ_g to a reduced value $\Delta_g = \Delta_0 \left(1 - \left(\frac{\Gamma}{\Delta_0} \right)^2 \right)^{3/2}$. The gap disappears completely at $\Gamma = 0.45 \Delta_0$, where Δ_0 is the order parameter in the absence of pair-breaking. The gapless superconductivity survives until the critical value $\Gamma_c = 0.5 \Delta_0$. This behavior is illustrated in Fig. 5(a), where we show the density of states as a function of energy for different values of Γ in units of Δ_0 . In Fig. 5(b) one can see the evolution of the order parameter and spectral gap with the depairing energy.

Let us discuss now how this modified density of states is reflected in the transport properties. In Fig. 6 we show I-Vs for different transmissions and different values of the depairing energy. The most noticeable features are: (i) the subharmonic gap structure is shifted to voltages $eV = 2 \Delta_g n$, and (ii) the subgap structure progressively disappears as the pair-breaking strength is increased. These features are simple consequences of the evolution of the density of states with Γ . Anyway, one can get a further insight by analyzing the contribution to the current of the individual MAR processes: $I_n = (2e/h) \int_0^{eV} dE P_n(E; V)$. These quantities are plotted in Fig. 7 for $T = 1$. As one can see, the threshold voltage for a n -order MAR is now $eV_n = \Delta_g n$ as a consequence of the reduced spectral gap. As the gap diminishes, the processes of lowest order dominate the I-Vs even at low bias. It is interesting to notice that even in a

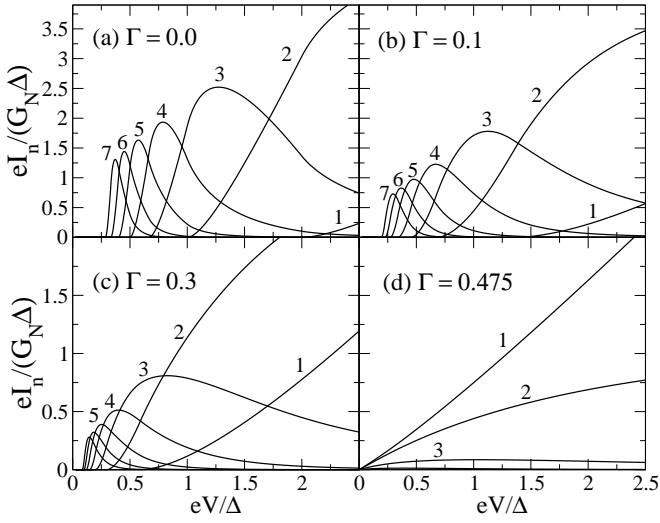


FIG. 7: Current contribution of processes $n = 1; 2; \dots$ for $T = 1$ as a function of voltage for superconductors with a depairing energy in units of Δ_0 . The current and the voltage have been normalized with the order parameter at the corresponding Γ . The order of the processes is indicated in the plots.

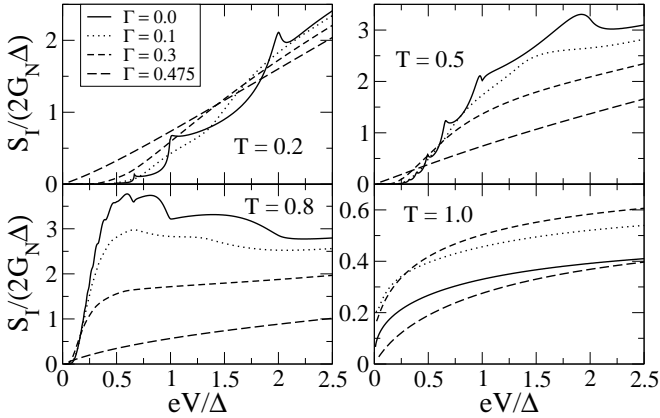


FIG. 8: Zero temperature noise for superconductors with a depairing energy in units of Δ_0 . The current and the voltage have been normalized with the order parameter at the corresponding Γ . The different panels correspond to different transmissions values.

gapless situation ($\Gamma = 0.475$) there is a finite contribution of the MARs. It is worth mentioning that in Refs. [67] and [68] the type of theory described here accounted for the magnetic field dependence of the I-Vs of atomic contacts.

Let us turn now our attention to the second and third cumulants that can be seen in Fig. 8 and Fig. 9, respectively. As in the case of the current, the subharmonic gap structure is shifted and smoothed as the gap evolves with Γ . Moreover, one can notice that for high transparencies and in the subgap region there is a great reduction of both cumulants as Γ increases. This is a consequence of the fact that low order MARs dominate even at low bias,

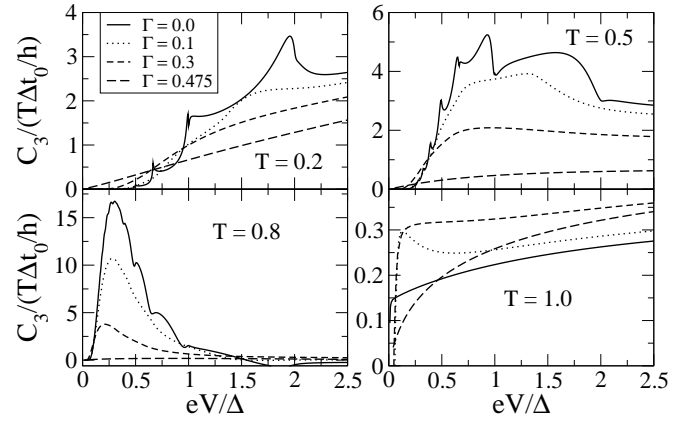


FIG. 9: Zero temperature third cumulant for superconductors with a depairing energy in units of Δ_0 . The current and the voltage have been normalized with the order parameter at the corresponding Γ . The different panels correspond to different transmissions values.

which in practice means that the charge transferred at these voltages is on average not very big.

C. Dissusive SNS contacts

So far we have discussed the case of a single channel contact. The results are trivially generalized to the multichannel case by introducing a sum over the conduction channels. In this subsection we briefly address the case of a short dissusive SNS junction with a large number of transmission channels and dissusive electron transport in the normal region. The superconducting leads are considered as BCS superconductors. In this case, the distribution of transmission coefficients is continuous, and it is characterized by the density function $\Gamma(T)$, which has the well-known bimodal form [69]

$$\Gamma(T) = \frac{G_N}{2G_0 T} \frac{1}{1 + \frac{1}{T}}; \quad (63)$$

where G_N is the normal-state conductance of the N region and $G_0 = 2e^2/h$ is the conductance quantum. Then, the different cumulants can be calculated from the single-channel results $C_n(T)$ as follows

$$C_n = \int_0^1 dT \Gamma(T) C_n(T); \quad (64)$$

In Fig. 10 (a) we show the first three cumulants for this SNS system. Both the current and the noise have previously discussed in the literature [22, 70], and here we recover these results. Both quantities exhibit a subharmonic gap structure which is a result of the competition of channels with different transparencies. Again, this structure can be understood by analyzing the individual contributions to the current of the different MARs,

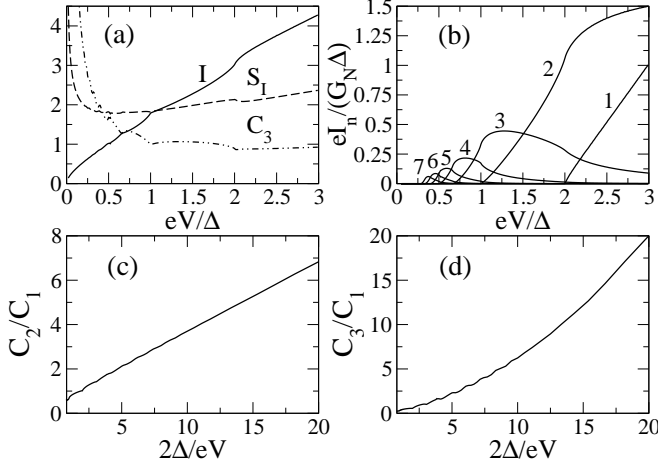


FIG. 10: Zero temperature transport properties of a short disordered SNS junction. (a) First three cumulants: current in units of (G_N/e) , shot noise in units of $(2G_N/e)$ and the third cumulant in units of (G_N/e) . (b) Current contribution of the different processes. (c) Ratio C_2/C_1 as a function of the inverse of the voltage. (d) Ratio C_3/C_1 as a function of the inverse of the voltage.

see Fig. 10(b). As one can see, at every voltage there are several processes giving a significant contributions, which makes that subgap structure much smoother than in the single-channel case. This fact also explains the absence of the charge quantization in this multichannel case. This is illustrated in Fig. 10(c), where we show the ratio C_2/C_1 as a measure of the effective charge. Notice that at low bias this effective charge grows as $(1/V)$ as obtained in Ref. [22]. In this regime the numerical results can be approximately described by the following linear function: $C_2/C_1 = 0.31(2/eV) + 0.55$. On the other hand, the third cumulant exhibits a huge increase at low voltages [35]. In particular, as shown in Fig. 10(d), the ratio C_3/C_1 grows as $(1/V)^2$ at low bias. In this regime the ratio can be approximated by $C_3/C_1 = 0.05(2/eV)^2 + 0.5$.

V. TRANSPORT PROPERTIES AT FINITE TEMPERATURES

So far we have discussed the transport properties of superconducting point contacts at zero temperature. In this section we shall investigate the role of the temperature, which we shall denote as T_e . We focus our attention to the case of a single channel contact between BCS superconductors. At finite temperature it is not easy to determine analytically the probabilities $P_n(E; V)$, and in this case we have calculated them numerically. The idea goes as follows. According to Eq. (18) we need to calculate the coefficients $P_n^0(E; V)$, which are simply the

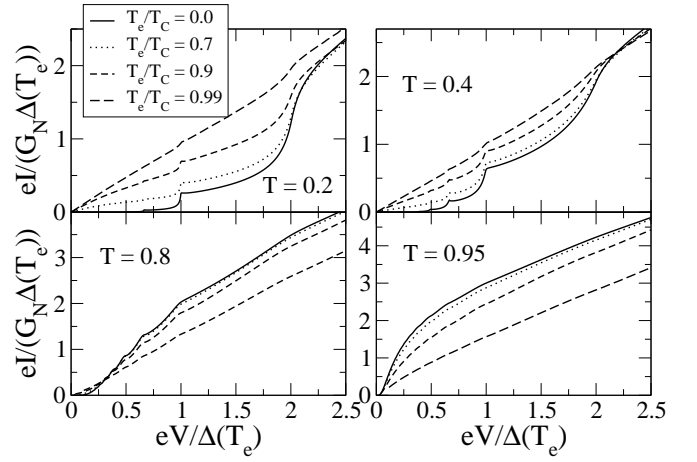


FIG. 11: Current-voltage characteristics at finite temperature for BCS superconductors. The temperature is in units of the critical temperature T_c . The current and the voltage are normalized with the temperature-dependent gap. The different panels correspond to different transmission values.

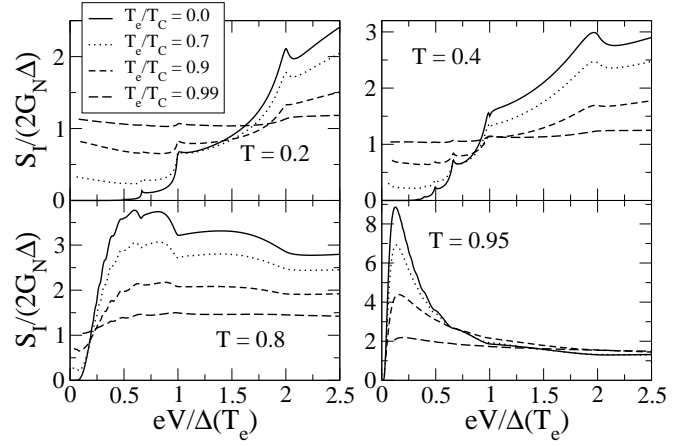


FIG. 12: Finite temperature noise for BCS superconductors. The temperature is normalized with the critical temperature T_c . The different panels correspond to different transmission values. The voltage is normalized with the temperature-dependent gap, and the current with the zero-temperature gap. Note that the scaling is different from the other plots in this section.

Fourier coefficients of the series in Eq. (18), i.e.

$$P_n^0(E; V) = \frac{1}{2} \int_0^{2\pi} d\theta e^{in\theta} \det Q(\theta) : \quad (65)$$

Finally, $\det Q(\theta)$ is calculated numerically. Of course, if one is only interested in the different cumulant, one can easily calculate them by taking the numerical derivative of the CGF, see Eq. 2.

In Figs. 11, 12, and 13 we show the current, noise and third cumulant, respectively, for different transmission and temperatures ranging from zero to the critical one. Notice that in order to get rid of the trivial temperature

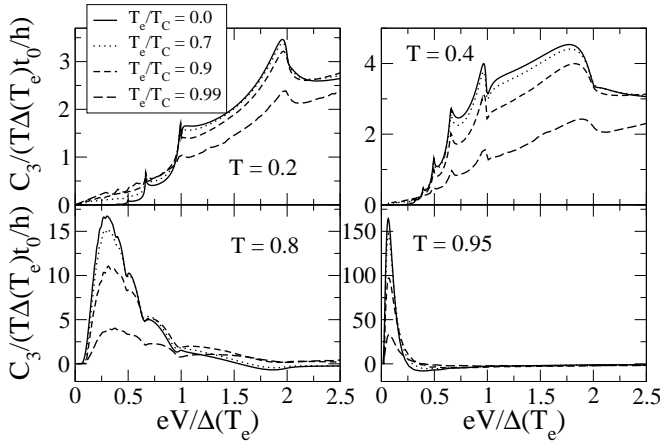


FIG. 13: Finite temperature third cumulant for BCS superconductors. The temperature is normalized with the critical temperature T_C . The different panels correspond to different transmission values. The third cumulant and the voltage are normalized with the temperature-dependent gap.

dependence due to the decrease of the gap we have normalized the voltage by the temperature-dependent gap

(T_e). As it can be seen in Fig. 11, the temperature progressively smoothes the SGS and increases the current for low transmissions. These are simple consequences of the thermal excitation of quasiparticles. For higher transmissions the temperature has the opposite effect (see the lower two panels in Fig. 11). The current decreases with increasing temperature and approaches the normal state current-voltage characteristic from above. At the same time the excess current, i.e. $I(V \rightarrow 0) - G_N V$, vanishes obviously. So in short, by increasing the temperature high-order Andreev reflections contribute less to the current, which is dominated by thermally activated direct quasiparticle tunneling. This behavior is clearly illustrated in Fig. 14, where we show the evolution with the temperature of the average probability $P_n(V) = (1/eV) \int_0^{eV} dE P_n(E; V)$ of different processes for a contact with transmission $T = 0.95$. Notice that we only show the first electron processes that give a positive contribution to the current. Remember that at finite temperature there are also hole processes that give a negative contribution to the current, the magnitude of which is still much smaller than the one of the electron processes in the shot noise limit $eV \ll k_B T$. At vanishing voltages, of course, $P_n = P_n$ as required by the fluctuation-dissipation theorem.

In Fig. 14 one can observe the following important features. First, at finite temperature the different processes do not have any finite threshold voltage, and they can contribute down to zero bias due to thermal activation. Second, as the temperature increases the probability of the single quasiparticle processes is greatly enhanced inside the gap. This fact results in a reduction of the average effective charge transmitted through the contact. Finally, notice that although the MAR probabilities are

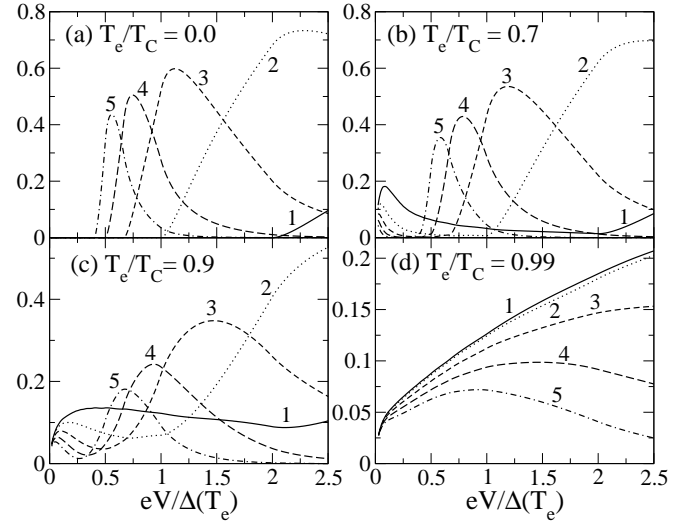


FIG. 14: Average MAR probabilities $P_n(V) = (1/eV) \int_0^{eV} dE P_n(E; V)$ at finite temperature as a function of voltage for a contact between BCS superconductors with transmission $T = 0.95$. The four panels correspond to different temperatures T_e expressed in units of the critical temperature T_C . The index of the processes is indicated in the plots.

reduced inside the gap at finite temperature, high-order processes can give a significant contribution to the transport even at voltages larger than the gap at the corresponding temperature. This is clearly at variance with the zero temperature case. To understand this behavior, let us recall that the total voltage gain for an order n process is neV , which means essentially that higher order processes can start well below the gap and end well above the gap. Now, at finite temperature e.g. the end states above the gap are filled with finite probability $f(E + neV)$, assuming that the process has started with a quasiparticle at energy E . A certain process can only happen if its final state is empty. This gives a factor $1 - f(E + neV)$, which enhances the chance for higher order processes, since they have to end up at higher energies, for which this factor is larger. On the other hand, a similar argument can be made about the initial state, which has to be filled for the process to take place. Again, this is more likely for higher order processes, since they can emerge from energies well below the gap, which are completely filled also at finite temperature.

It is interesting to discuss the qualitative different temperature behavior of the second and third cumulants. The noise exhibits a transition from pure shot noise at zero temperature to thermal noise when the temperature is larger than the voltage. As it can be seen in Fig. 12, this transition is reflected in a saturation of the noise at low bias to a finite value, which is given by the fluctuation-dissipation theorem. It is interesting to note, that the noise decreases as a function of voltage in the transition region from thermal to shot noise also for relatively small transmissions. Such a behavior can be at-

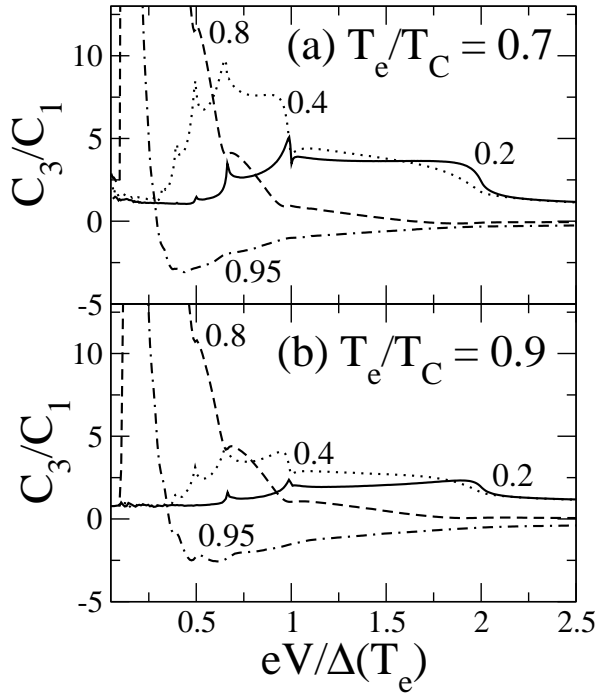


FIG. 15: Ratio C_3/C_1 for two different temperatures as a function of the voltage for a contact between BCS superconductors. The different curves correspond to different transmissions as indicated in the plots.

tributed to the multinomial distribution. Interestingly, from Eq. (28) we see that the correlations between processes of orders with opposite sign (e.g. $m = -n$) tend to increase the noise. As these terms appear only if the respective probabilities are non-negligible, the reduction of noise below the thermal level can be understood as consequence of the vanishing cross correlations between processes of orders with different signs.

The temperature dependence of the third cumulant is very interesting. First we recall that the third cumulant vanishes at zero voltage for any temperature (as all odd cumulants do). In Ref. [45] the temperature dependence of the third cumulant for a quantum contact between normal metals was calculated. It was shown, that an increasing transparency has quite a dramatic effect on the third cumulant. For a tunnel junction (i.e. for small transmission) C_3 is independent of the temperature and it is simply equal to the $q^2 C_1$. However, this is interesting because it allows a direct measurement of the charge q transferred in an elementary event even for voltages below the shot noise limit. Note, that this relation holds also for non-linear current-voltage characteristics, since it is a consequence of the bidirectional Poisson distribution in this limit. The effects of a finite transparency are even more dramatic. The third cumulant has a marked temperature dependence, crossing over from a FI dependence, where $F = 1 - T$ is the Fano factor, to a novel high-temperature dependence $F I(1 - 2T)$, which can even become negative for $T > 1/2$. In view of these find-

ings, we will now discuss our results for the temperature dependence of the third cumulant of a superconducting point contact.

First, we note that in Fig. 13 C_3 has a temperature dependence even in the tunnel regime. As explained in the previous paragraph, this in contrast with the normal state, where C_3 is almost independent of the temperature, as it has been discussed theoretically in Ref. [45] and observed experimentally in Ref. [71]. In our case the temperature dependence is due to the change in the MAR probabilities caused by the thermal activation. As explained above, the thermal activation enhances the probability of the tunneling of single quasiparticles inside the gap, which in turn reduces the average effective charge. A consequence of this fact is the great reduction of the ratio C_3/C_1 as the temperature increases. This is illustrated in Fig. 15. This reduction is specially dramatic in the subgap region for high transparencies, as it can be seen directly in Fig. 13.

VI. CONCLUSIONS

We have presented a detailed analysis of the full counting statistics in superconducting point contacts at finite bias voltage. We have demonstrated that the charge transfer in these systems is described by a multinomial distribution of processes, in which multiple charges n (with $n = 1; 2; 3; \dots; 20; \dots$) are transferred through the contact. These processes are nothing but multiple Andreev reflections. The knowledge of the full counting statistics allows us to obtain the probabilities of the individual MARs, providing so a deep insight into the electronic transport of these junctions. From the knowledge of these probabilities one can easily calculate not only the current or the noise, but all the cumulants of the current distribution. We have also shown that one can obtain analytical expressions for the MAR probabilities at zero temperature, which provides the most efficient method to calculate the transport properties of these contacts. Moreover, the FCS approach allows us to describe a great variety of situations in a unified manner.

In this sense, we have addressed different situations such as contacts between BCS superconductors, junctions between superconductors where a pair-breaking mechanism is acting or short diffusive SNS contacts. We have also discussed the temperature dependence of the first cumulants and illustrated their peculiarities as compared with the normal case. It is also worth mentioning that the formalism developed in this work can be easily applied to other situations not addressed here such as point contacts with proximity-effect superconductors [72] and Josephson junctions of unconventional superconductors [73, 74].

From the full counting statistics view, we have found a new distribution occurring in superconducting point contacts. The statistics takes the form of a multinomial distribution of charge transfers of all orders, which are

allowed by the applied bias voltage. We have shown, that the limit of opaque contacts provides an interesting situation, in which Poissonian statistics makes it possible to observe multiple charge transfers in a direct manner. Furthermore, we have discussed consequences of the multinomial statistics of charge transfers of different sizes at the same time. For example, an open contact has a finite noise due to the presence of different MAR processes at the same time. The temperature dependence of the counting statistics provides a new insight in the transport characteristic, since we have shown that higher order Andreev processes contribute also at voltages much larger than the superconducting gap.

Finally we remark, that the FCS approach provides a

fresh view of the electronic transport of superconducting point contacts and it seems to be a natural choice for future theoretical analyses. On the other side, superconducting contacts show an interesting new counting statistics, namely a multinomial distribution, and we expect further interesting results in other superconducting systems out of equilibrium.

We acknowledge discussions with A. Levy Yeyati, A. Mart n-Rodero and Yu.V. Nazarov. JCC was financially supported by the DFG within the CFN and by the Helmholtz Gemeinschaft within the Nachwuchsgruppe program (contract VH-NG-029), and WB by the Swiss NSF and the NCCR Nanoscience.

-
- [1] I. Giaever, H.R. Hart, Jr., and K. Magerle, *Phys. Rev.* **126**, 941 (1962).
 - [2] J. Bardeen, L.N. Cooper, and J.R. Schrieffer, *Phys. Rev.* **108**, 1175 (1957).
 - [3] B.N. Taylor and E. Burstein, *Phys. Rev. Lett.* **10**, 14 (1963).
 - [4] I.K. Yanson, V.M. Svistunov, and I.M. Dmitrenko, *Sov. Phys. JETP* **20**, 1404 (1965).
 - [5] S.M. Marcus, *Phys. Letters* **19**, 623 (1966); **20**, 236 (1966).
 - [6] J.M. Rowell and W.L. Feldmann, *Phys. Rev.* **172**, 393 (1968).
 - [7] A.A. Bright and J.R. Merrill, *Phys. Rev.* **184**, 446 (1969).
 - [8] I. Giaever and H.R. Zeller, *Phys. Rev. B* **1**, 4278 (1970).
 - [9] J.R. Schrieffer and J.W. Wilkins, *Phys. Rev. Lett.* **10**, 17 (1963).
 - [10] N.R. Werthamer, *Phys. Rev.* **147**, 255 (1966).
 - [11] T.M. Klapwijk, G.E. Blonder and M. Tinkham, *Physica B* **109& 110**, 1657 (1982).
 - [12] M. Octavio, G.E. Blonder, M. Tinkham, and T.M. Klapwijk, *Phys. Rev. B* **27**, 6739 (1983).
 - [13] K. Flensberg, J.B. Hansen and M. Octavio, *Phys. Rev. B* **38**, 8707 (1988).
 - [14] G.B. Arnold, *J. Low Temp. Phys.* **68**, 1 (1987).
 - [15] E.N. Bratus, V.S. Shumeiko, and G. Wendin, *Phys. Rev. Lett.* **74**, 2110 (1995).
 - [16] D. Averin and A. Bardas, *Phys. Rev. Lett.* **75**, 1831 (1995).
 - [17] M. Hurd, S. Datta and P.F. Bagwell, *Phys. Rev. B* **54**, 6557 (1996).
 - [18] J.C. Cuevas, A. Mart n-Rodero and A. Levy Yeyati, *Phys. Rev. B* **54**, 7366 (1996).
 - [19] A. Levy Yeyati, J.C. Cuevas, A. Lopez-Davalos, and A. Mart n-Rodero, *Phys. Rev. B* **55**, 6317 (1997).
 - [20] G. Johansson, E.N. Bratus, V.S. Shumeiko, and G. Wendin, *Phys. Rev. B* **60**, 1382 (1999).
 - [21] J.C. Cuevas, A. Mart n-Rodero and A. Levy Yeyati, *Phys. Rev. Lett.* **82**, 4086 (1999).
 - [22] Y. Naveh and D.V. Averin, *Phys. Rev. Lett.* **82**, 4090 (1999).
 - [23] J.C. Cuevas, J. Heinrich, A. Mart n-Rodero, A. Levy Yeyati, G. Schon, *Phys. Rev. Lett.* **88**, 157001 (2002).
 - [24] C.J.M. Muller, J.M. van Ruitenbeek, and L.J. de Jongh, *Phys. Rev. Lett.* **69**, 140 (1992).
 - [25] N. van der Post, E.T. Peters, I.K. Yanson, and J.M. van Ruitenbeek, *Phys. Rev. Lett.* **73**, 2611 (1994).
 - [26] J.G. Rodrigo, N. Agrat, C. Sirvent and S. Vieira, *Phys. Rev. B* **50**, 12788 (1994).
 - [27] M.C. Kooops, G.V. van Duyneveldt, and R. de Bruyn Ouboter, *Phys. Rev. Lett.* **77**, 2542 (1996).
 - [28] E. Scheer, P. Joyez, D. Esteve, C. Urbina and M.H. Devoret, *Phys. Rev. Lett.* **78**, 3535 (1997).
 - [29] E. Scheer, N. Agrat, J.C. Cuevas, A. Levy Yeyati, B. Ludoph, A. Mart n-Rodero, G. Rubio, J.M. van Ruitenbeek and C. Urbina, *Nature* **394**, 154 (1998).
 - [30] B. Ludoph et al., *Phys. Rev. B* **61**, 8561 (2000).
 - [31] M.F. Goman et al., *Phys. Rev. Lett.* **85**, 170 (2000).
 - [32] R. Cron et al., *Phys. Rev. Lett.* **86**, 4104 (2001).
 - [33] M. Buitelaar, W. Belzig, B. Babic, Th. Nussbaumer, C. Bruder, and C. Schonenberger, *Phys. Rev. Lett.* **91**, 057005 (2003).
 - [34] J.C. Cuevas and W. Belzig, *Phys. Rev. Lett.* **91**, 187001 (2003).
 - [35] G. Johansson, P. Samuelsson and A. Ingemar, *Phys. Rev. Lett.* **91**, 187002 (2003).
 - [36] L. Mandel and E. Wolf, *Optical Coherence and Quantum Optics* (Cambridge University, Cambridge, England, 1995).
 - [37] L.S. Levitov and G.B. Lesovik, *Pis'ma Zh. Eksp. Teor. Fiz.* **58**, 225 (1993); L.S. Levitov, H.W. Lee, and G.B. Lesovik, *J. Math. Phys.* **37**, 4845 (1996).
 - [38] *Quantum Noise in Mesoscopic Physics*, edited by Yu.V. Nazarov (Kluwer, Dordrecht, 2003).
 - [39] L.S. Levitov, H.W. Lee, and G.B. Lesovik, *J. Math. Phys.* **37**, 4845 (1996).
 - [40] H. Lee, L.S. Levitov, and A.Yu. Yakovets, *Phys. Rev. B* **51**, 4079 (1996).
 - [41] Yu.V. Nazarov, *Ann. Phys. (Leipzig)* **8**, SI-193 (1999).
 - [42] O.N. Dorokhov, *Solid State Comm.* **51**, 381 (1984).
 - [43] Yu.V. Nazarov, *Phys. Rev. Lett.* **73**, 1420 (1994).
 - [44] R. de Picciotto, M. Reznikov, M. Heiblum, V. Umansky, G. Bunin and D. Mahalu, *Nature* **389**, 162 (1997); L. Saminadayar, D.C. Glatelli, Y. Jin and B. Etienne, *Phys. Rev. Lett.* **79**, 2526 (1997); M. Reznikov, R. de Picciotto, T.G. Griths, M. Heiblum, and V. Umansky, *Nature* **399**, 238 (1999); T.G. Griths, E. Comfari, M. Heiblum, A. Stern, V. Umansky, *Phys. Rev. Lett.* **85**, 3918 (2000).

- [45] L.S. Levitov and M. Reznikov, cond-mat/0111057.
- [46] H. Saleur and U. Weiss, Phys. Rev. B 63, 201302 (2001).
- [47] W. Belzig and Yu. V. Nazarov, Phys. Rev. Lett. 87, 197006 (2001).
- [48] B. A. Muzykantskii and D. E. Khamelnitzkii, Phys. Rev. B 50, 3982 (1994).
- [49] C. W. J. Beenakker, Phys. Rev. B 46, 12841 (1992); C. J. Lambert, J. Phys. Condens. Matter 3, 6579; Y. Takane and H. Ebisawa, J. Phys. Soc. Jpn. 61, 1685 (1992).
- [50] W. Belzig in [38].
- [51] W. Belzig and P. Samuelsson, Europhys. Lett. 64, 253 (2003).
- [52] P. Samuelsson, W. Belzig, and Yu. V. Nazarov, Phys. Rev. Lett. 92, 196807 (2004).
- [53] W. Belzig and Yu. V. Nazarov, Phys. Rev. Lett. 87, 067006 (2001).
- [54] B. Reulet, A. A. Kozhevnikov, D. E. Prober, W. Belzig, and Yu. V. Nazarov, Phys. Rev. Lett. 90, 066601 (2003).
- [55] X. Jehl, P. Payet-Burin, C. Baraduc, R. Calemczuk, and M. Sanquer, Phys. Rev. Lett. 83, 1660 (1999); A. A. Kozhevnikov, R. J. Schoelkopf, and D. E. Prober, Phys. Rev. Lett. 84, 3398 (2000); X. Jehl, M. Sanquer, R. Calemczuk, and D. Mailly, Nature 405, 50 (2000).
- [56] M. J. M. de Jong and C. W. J. Beenakker, Phys. Rev. B 49, 16070 (1994); K. E. Nagaev and M. Buttiker, ibid. 63, 081301(R) (2001).
- [57] F. Leoch, C. Homann, M. Sanquer, and D. Quirion, Phys. Rev. Lett. 90, 067002 (2003).
- [58] M. P. V. Stenberg and T. T. Heikkilä, Phys. Rev. B 66, 144504 (2002).
- [59] F. Pistolesi, G. Bignon, and F. W. J. Hekking, cond-mat/0303165 (unpublished).
- [60] Yu. V. Nazarov and M. K. Indermann, Eur. Phys. J. B 35, 413 (2003).
- [61] M. K. Indermann and Yu. V. Nazarov, in Ref. [38].
- [62] Alessandro Romito and Yu. V. Nazarov, cond-mat/0402412.
- [63] Yu. V. Nazarov, Superlattices Microsc. 25, 1221 (1999).
- [64] A. Shelankov and J. Rammer, Europhys. Lett. 63, 485 (2003).
- [65] K. Maki, in Superconductivity, edited by R. D. Parks (Marcel Dekker, New York, 1969), p.1035.
- [66] S. Skalski, O. Betbeder-Matibet, P. R. Weiss, Phys. Rev. 136, A1500 (1964).
- [67] E. Scheer, J. C. Cuevas, A. Levy Yeyati, A. Martn-Rodero, P. Joyez, M. H. Devoret, D. Esteve, C. Urbina, Physica B 280, 425 (2000).
- [68] H. Suderow, E. Bascones, W. Belzig, F. Guinea, and S. Vieira, Europhys. Lett. 50, 749 (2000).
- [69] Yu. V. Nazarov, Phys. Rev. Lett. 73, 134 (1994).
- [70] A. Bardas and D. V. Averin, Phys. Rev. B 56, R8518 (1997).
- [71] B. Reulet, J. Senzier, D. E. Prober, Phys. Rev. Lett. 91, 196601 (2003).
- [72] E. Scheer, W. Belzig, Y. Naveh, M. H. Devoret, D. Esteve, and C. Urbina, Phys. Rev. Lett. 86, 284 (2001).
- [73] A. Poenicke, J. C. Cuevas and M. Fogelstrom, Phys. Rev. B 65, 220510 (2002).
- [74] J. C. Cuevas and M. Fogelstrom, Phys. Rev. Lett. 89, 227003 (2002).
- [75] This relation follows from the definition of the current noise power $S_I = 2 \int_{-\infty}^{\infty} d\hbar I(\hbar=2)I(\hbar=2)i$. The second cumulant, on the other hand, is defined by $C_2 = \int_{-\infty}^{\infty} dt d\hbar I(\hbar=2)I(\hbar=2)i$. In the static situation the current-current correlation function depends only on the time difference $\hbar = t - t'$ and decays on some characteristic scale τ_0 . For long observation times $t_0 \gg \tau_0$ we find for the second cumulant $C_2 = (\tau_0=2e^2)S_I$.